Modeling and Control of a HSM Machine Tool With Parallel Kinematics

B. C. Bouzgarrou
P.Ray
G. Gogu
LaRAMA-IFMA
Campus de Clermont-Fd, BP-265
63175 Aubière, France.
bouzgarrou@ifma.fr

B. Thuilot
LASMEA
24, avenue des Landais
63177 Aubière, France.
Benoit.Thuilot@lasmea.univ-bpclermont.fr

Abstract

Machine tools are designed to reach a given performance level in term of precision and static and dynamic stiffness. In this article, we present the modeling and control of a high speed machining and working machine tool prototype, with parallel kinematic architecture. Required speeds and accelerations make that flexibility and adopted control strategy have to be considered in dimensioning. Rigid and lumped flexibilities dynamic models are derived. A non-linear control strategy is adopted, based on rigid dynamic model. The control validity and the importance of taking into account flexibility are illustrated by simulation results.

1 Introduction

The increasing evolution of machine tools speed and acceleration leads to a dynamic behavior in which flexibility cannot be ignored. Deriving dynamic model taking into account flexibility is very useful for mechanical parts dimensioning as well as for control design.

The use of parallel kinematics and the development of new control systems are among research areas to which high speed machining (HSM) is oriented these last years [2] [10]. Parallel kinematics allows to reduce moving masses and to increase manipulator stiffness. Thereafter, higher speed and acceleration are reachable. P.I.D. feedback strategy is commonly used for machine tool axes control. Advanced control systems use feedforward action to improve tracking performances [1].

In the second section of this article, we present rigid and flexible dynamic modeling of the machine. Elastic behavior is approached by introducing lumped flexibility at guideway components locations. Section 3 is devoted to control design. It relies mainly on rigid dynamic model. The flexible one is used to cancel the static gravity effects introduced by the flexibilities. Proposed control strategy is finally validated by simulation results and compared to P.I.D. controller.

2 Dynamic model

In this article, we consider a 3 degrees of mobility HSM machine tool prototype with parallel kinematic architecture, Fig. (1). It is destined for milling operations. Motion in the XY plane is performed by a 2 degrees of mobility parallel mechanism on which the Z axis is embarked. Only prismatic joints are actuated with linear synchronous motors. Such actuation system provides higher stiffness and accuracy than ball screw drive. The considered machine links are related by prismatic and revolute joints which axes are parallel or perpendicular, Fig (1). Therefore, TCS method [8], is applicable for geometric modeling. Two frames are used for each link i, $A_i(\vec{x}_i, \vec{y}_i, \vec{z}_i)$ and $A_{i'}(\vec{x}_{i'}, \vec{y}_{i'}, \vec{z}_{i'})$. The relative configuration of these frames is given by a constant 4×4 shape matrix $\mathbf{F}_i$. Machine configuration is described by 6 joint variables given by $\mathbf{q} = \left[\begin{array}{cccccc} s_{21} & s_{65} & s_{32} & s_{54} & \phi_{10} & \phi_{60} \end{array} \right]^T$. $b_1 \ldots b_6$ are constant geometrical parameters. The configuration of the tool is given by the position and the orientation coordinate system $E(\vec{x}_3, \vec{y}_3, \vec{z}_3)$.

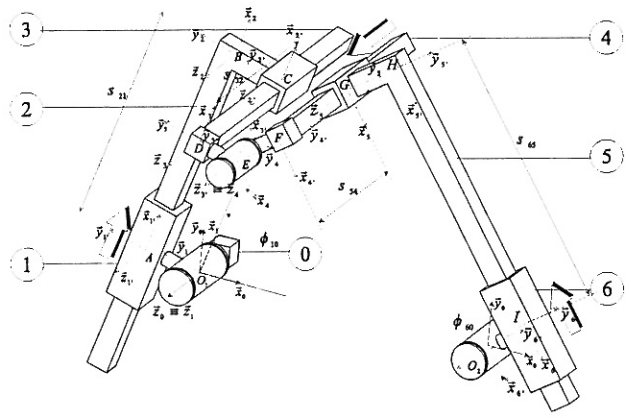

Figure 1: 3 degrees of mobility parallel manipulator: TCS parameters

2.1 Rigid model

Considered machine has closed kinematic chain. The formulation of the equations of motion can be performed according to a set of independent coordinates, $\mathbf{s} = \left[\begin{array}{ccc} s_{21} & s_{65} & s_{32} \end{array}\right]^T$, and a set of dependent coordinates $\boldsymbol{\phi} = \left[\begin{array}{ccc} s_{54} & \phi_{10} & \phi_{60} \end{array}\right]^T$. In that case, Lagrange equations with multipliers are used. We denote by $L = T - V$ the Lagrangian of the mechanical system, T and V are respectively kinetic and potential energy. Kinematic constraints are defined by $\boldsymbol{\Phi}(\mathbf{q}) = \mathbf{0}$. Equations governing the motion are given by:

$$\begin{array}{rcl} \dfrac{d}{dt}\left(\dfrac{\partial L}{\partial \dot{\mathbf{q}}}\right) - \dfrac{\partial L}{\partial \mathbf{q}} + \boldsymbol{\Phi}_q^T \boldsymbol{\lambda} & = & \mathbf{Q} + \mathbf{S} \\ \boldsymbol{\Phi}(\mathbf{q}) & = & \mathbf{0} \end{array} \qquad (1)$$

where $\boldsymbol{\Phi}_q = (\partial \boldsymbol{\Phi} / \partial \mathbf{q})$ is a 3×6 matrix, $\boldsymbol{\lambda}$ is the 3×1 vector of Lagrange multipliers and $\mathbf{Q}$ is the 6×1 vector of generalized forces. $\mathbf{S} = \left[\begin{array}{cc} \mathbf{u}^T & \mathbf{0} \end{array}\right]^T$, $\mathbf{u}$ is the 3×1 vector of control forces applied by the linear motors. Rigid dynamic model can be expressed as follows

$$\begin{array}{c} \left[\begin{array}{cc} \mathbf{M}_{ss} & \mathbf{M}_{s\phi} \\ \mathbf{M}_{s\phi}^T & \mathbf{M}_{\phi\phi} \end{array}\right] \left[\begin{array}{c} \ddot{\mathbf{s}} \\ \ddot{\boldsymbol{\phi}} \end{array}\right] + \left[\begin{array}{cc} \mathbf{C}_{ss} & \mathbf{C}_{s\phi} \\ \mathbf{C}_{\phi s} & \mathbf{C}_{\phi\phi} \end{array}\right] \left[\begin{array}{c} \dot{\mathbf{s}} \\ \dot{\boldsymbol{\phi}} \end{array}\right] \\ + \left[\begin{array}{c} \mathbf{g}_s \\ \mathbf{g}_\phi \end{array}\right] + \left[\begin{array}{c} \boldsymbol{\Phi}_s^T \\ \boldsymbol{\Phi}_\phi^T \end{array}\right] \boldsymbol{\lambda} = \left[\begin{array}{c} \mathbf{u} + \mathbf{Q}_s \\ \mathbf{Q}_\phi \end{array}\right] \end{array} \qquad (2)$$

$\mathbf{M}_{ij}$, $\mathbf{C}_{ij}$, $\boldsymbol{\Phi}_i$, $\mathbf{g}_i$ and $\mathbf{Q}_i$, $(i, j \in \{s, \phi\})$ are respectively sub-matrices of mass, centrifugal and Coriolis terms, constraints, gravity forces and external and non-conservatives internal generalized forces. The size of these sub-matrices and vectors corresponds to the partition defined for generalized coordinates.

2.2 Lumped flexibility model

Structural flexibility is a performance limitation factor in HSM. Several works have treated the modeling of flexible manipulators [3] [9]. Derived models are reduced to a set of degrees of freedom obtained by modal truncation [12], or approached by lumped flexibility [11]. This last approach is useful to obtain simple but accurate enough model at the design stage. We consider lumped flexibility at the location of linear guideway components connecting links 1 and 2 and links 5 and 6, Fig. (1). This choice is motivated by finite element analysis performed in previous works [5]. When flexible link is considered, the relative configuration of frames $A_i(\vec{x}_i, \vec{y}_i, \vec{z}_i)$ and $A_{i'}(\vec{x}_{i'}, \vec{y}_{i'}, \vec{z}_{i'})$ is given by $\mathbf{F}_i \boldsymbol{\Delta}_i$. Where $\boldsymbol{\Delta}_i$ is a 4×4 infinitesimal displacement matrix that describes deflections [8]. $\boldsymbol{\Delta}_i$ is associated to infinitesimal displacement vector $\boldsymbol{\delta}_i = \left[\begin{array}{cccccc} d_{xi} & d_{yi} & d_{zi} & \delta_{xi} & \delta_{yi} & \delta_{zi} \end{array}\right]^T$. Thereafter, in our case, manipulator generalized coordinates are augmented by a set of flexible coordinates given by the vector $\boldsymbol{\delta} = \left[\begin{array}{cc} \boldsymbol{\delta}_2 & \boldsymbol{\delta}_5 \end{array}\right]^T$. Potential elastic energy is calculated by 12×12 stiffness matrix $\mathbf{K}_\delta$ which depends on lumped stiffness values and manipulator configuration. The dynamic model of the flexible manipulator has the following form [4]

$$\begin{array}{c} \left[\begin{array}{ccc} \mathbf{M}_{ss} & \mathbf{M}_{s\phi} & \mathbf{M}_{s\delta} \\ \mathbf{M}_{s\phi}^T & \mathbf{M}_{\phi\phi} & \mathbf{M}_{\phi\delta} \\ \mathbf{M}_{s\delta}^T & \mathbf{M}_{\phi\delta}^T & \mathbf{M}_{\delta\delta} \end{array}\right] \left[\begin{array}{c} \ddot{\mathbf{s}} \\ \ddot{\boldsymbol{\phi}} \\ \ddot{\boldsymbol{\delta}} \end{array}\right] + \\ \left[\begin{array}{ccc} \mathbf{C}_{ss} & \mathbf{C}_{s\phi} & \mathbf{C}_{s\delta} \\ \mathbf{C}_{\phi s} & \mathbf{C}_{\phi\phi} & \mathbf{C}_{\phi\delta} \\ \mathbf{C}_{\delta s} & \mathbf{C}_{\delta\phi} & \mathbf{C}_{\delta\delta} \end{array}\right] \left[\begin{array}{c} \dot{\mathbf{s}} \\ \dot{\boldsymbol{\phi}} \\ \dot{\boldsymbol{\delta}} \end{array}\right] + \\ \left[\begin{array}{ccc} 0 & 0 & 0 \\ 0 & 0 & 0 \\ 0 & 0 & \mathbf{K}_\delta \end{array}\right] \left[\begin{array}{c} \mathbf{s} \\ \boldsymbol{\phi} \\ \boldsymbol{\delta} \end{array}\right] + \\ \left[\begin{array}{c} \mathbf{g}_s \\ \mathbf{g}_\phi \\ \mathbf{g}_\delta \end{array}\right] + \left[\begin{array}{c} \boldsymbol{\Phi}_s^T \\ \boldsymbol{\Phi}_\phi^T \\ \boldsymbol{\Phi}_\delta^T \end{array}\right] \boldsymbol{\lambda} = \left[\begin{array}{c} \mathbf{u} + \mathbf{Q}_s \\ \mathbf{Q}_\phi \\ \mathbf{Q}_\delta \end{array}\right] \end{array} \qquad (3)$$

3 Control

Control design is mainly based on rigid dynamic model. The flexible model is used to cancel the static gravity effects introduced by the flexibilities. It also allows control validation and performance limitations checking.

3.1 P.I.D. controller

P.I.D. controller is based on two cascade position and speed loops, Fig. (2). It is commonly used for machine tool axes control. Current loop is considered to be fast enough and was not studied in this article.

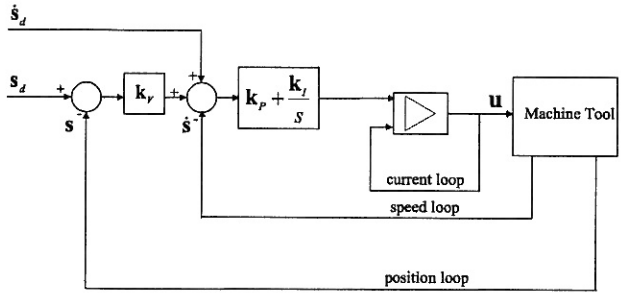

Figure 2: P.I.D. Controller

$\mathbf{k}_V$ is the proportional gain matrix of the P. position loop, $\mathbf{k}_P$ and $\mathbf{k}_I$ are respectively the proportional and integral gain matrices of the P.I. speed loop. $\mathbf{s}_d$ and $\dot{\mathbf{s}}_d$ are time variant joint space desired positions and velocities.

3.2 Computed torque control

P.I.D. controller does not allow to have uniform performance, in term of dynamic response and precision, on all the working space since machine dynamic behavior is highly non linear. The use of a computed torque control (or inverse dynamics control) is well known in robotics and consists in linearizing and decoupling equations of motion [7]. We propose the adaptation of this control strategy to manipulators with parallel kinematics. At first stage, we eliminate Lagrange multipliers using Eq. (2). Singularity analysis shows that the 3×3 matrix $\mathbf{\Phi}_\phi$ is invertible on all the prescribed work space [6].We can write

$$\begin{aligned}\lambda &= \left(\mathbf{\Phi}_\phi^T\right)^{-1}(\mathbf{Q}_\phi - \\ &\left(\mathbf{M}_{s\phi}^T\ddot{\mathbf{s}} + \mathbf{M}_{\phi\phi}\ddot{\boldsymbol{\phi}} + \mathbf{C}_{\phi s}\dot{\mathbf{s}} + \mathbf{C}_{\phi\phi}\dot{\boldsymbol{\phi}} + \mathbf{g}_\phi\right))\end{aligned} \tag{4}$$

To eliminate dependent coordinates, time differentiation of constraint equation $\mathbf{\Phi}(\mathbf{q}) = \mathbf{0}$ is performed. We obtain following expressions

$$\begin{aligned}\dot{\boldsymbol{\phi}} &= -\mathbf{\Phi}_\phi^{-1}\mathbf{\Phi}_s\dot{\mathbf{s}} \\ \ddot{\boldsymbol{\phi}} &= -\mathbf{\Phi}_\phi^{-1}\left(\mathbf{\Phi}_s\ddot{\mathbf{s}} + \dot{\mathbf{\Phi}}_s\dot{\mathbf{s}} + \dot{\mathbf{\Phi}}_\phi\dot{\boldsymbol{\phi}}\right)\end{aligned} \tag{5}$$

By using Eq. (2), (4) and (5), we obtain joint space dynamic model

$$\mathbf{M}_S\ddot{\mathbf{s}} + \mathbf{C}_S\dot{\mathbf{s}} + \mathbf{G}_S = \mathbf{u} + \mathbf{Q}_s \tag{6}$$

with

$$\begin{aligned}\mathbf{M}_S = {} & \mathbf{M}_{ss} - \mathbf{M}_{s\phi}\mathbf{\Phi}_\phi^{-1}\mathbf{\Phi}_s - \mathbf{\Phi}_s^T\left(\mathbf{\Phi}_\phi^T\right)^{-1}\mathbf{M}_{s\phi}^T \\ & + \mathbf{\Phi}_s^T\left(\mathbf{\Phi}_\phi^T\right)^{-1}\mathbf{M}_{\phi\phi}\mathbf{\Phi}_\phi^{-1}\mathbf{\Phi}_s \\ \mathbf{C}_s = {} & -\mathbf{M}_{s\phi}\mathbf{\Phi}_\phi^{-1}\left(\dot{\mathbf{\Phi}}_s - \dot{\mathbf{\Phi}}_\phi\mathbf{\Phi}_\phi^{-1}\mathbf{\Phi}_s\right) + \mathbf{C}_{ss} \\ & - \mathbf{C}_{s\phi}\mathbf{\Phi}_\phi^{-1}\mathbf{\Phi}_s + \mathbf{\Phi}_s^T\left(\mathbf{\Phi}_\phi^T\right)^{-1} \\ & \left(\mathbf{M}_{\phi\phi}\left(\dot{\mathbf{\Phi}}_s - \dot{\mathbf{\Phi}}_\phi\mathbf{\Phi}_\phi^{-1}\mathbf{\Phi}_s\right) - \mathbf{C}_{\phi s} + \mathbf{C}_{\phi\phi}\mathbf{\Phi}_\phi^{-1}\mathbf{\Phi}_s\right) \\ \mathbf{G}_S = {} & \mathbf{g}_s - \mathbf{\Phi}_s^T\left(\mathbf{\Phi}_\phi^T\right)^{-1}(\mathbf{g}_\phi - \mathbf{Q}_\phi)\end{aligned}$$

Now we can apply classical inverse dynamics control law given by

$$\mathbf{u} = \mathbf{u}_0 + \mathbf{C}_S\dot{\mathbf{s}} + \mathbf{G}_S - \mathbf{Q}_s \tag{7}$$

by adopting

$$\mathbf{u}_0 = \mathbf{M}_S\left(\ddot{\mathbf{s}}_d + \mathbf{K}_D\left(\dot{\mathbf{s}}_d - \dot{\mathbf{s}}\right) + \mathbf{K}_P\left(\mathbf{s}_d - \mathbf{s}\right) + \mathbf{K}_I\int_0^t\left(\left(\mathbf{s}_d - \mathbf{s}\right)d\tau\right)\right) \tag{8}$$

We obtain the closed loop dynamics of the rigid manipulator

$$\ddot{\mathbf{e}} + \mathbf{K}_D\dot{\mathbf{e}} + \mathbf{K}_P\mathbf{e} + \mathbf{K}_I\int_0^t\mathbf{e}\,d\tau = \mathbf{0} \tag{9}$$

where $\mathbf{s}_d$, $\dot{\mathbf{s}}_d$ and $\ddot{\mathbf{s}}_d$ are joint space desired trajectory and its successive time derivatives. $\mathbf{e} = \mathbf{s}_d - \mathbf{s}$ is the joint space tracking error. $\mathbf{K}_D$, $\mathbf{K}_P$ and $\mathbf{K}_I$ are respectively derivative, proportional and integral definite positive gain matrices. One can adopt $\mathbf{K}_D = k_d\mathbf{I}_3$, $\mathbf{K}_P = k_p\mathbf{I}_3$ and $\mathbf{K}_I = k_i\mathbf{I}_3$ where $\mathbf{I}_3$ is 3×3 identity matrix.

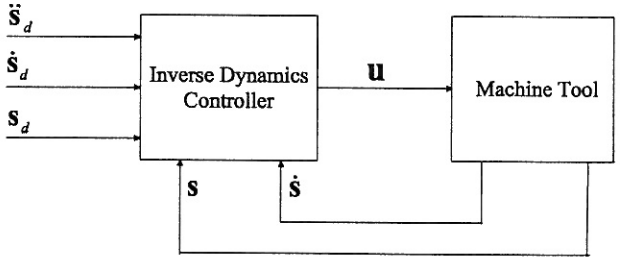

Figure 3: Inverse Dynamics Controller

3.3 Gravity compensation

We denote by $\mathbf{x}_d$ the desired static equilibrium position. $\mathbf{s}_r$ is the desired joint configuration satisfying $\mathbf{x}_d = \mathbf{G}_r(\mathbf{s}_r)$, where $\mathbf{G}_r$ is the forward geometric model of the rigid manipulator. We denote by $\mathbf{J}_r$ the Jacobian matrix satisfying $\dot{\mathbf{x}} = \mathbf{J}_r\dot{\mathbf{s}}$, for rigid manipulator. Structure deformation under gravity causes end-effector (tool) position error. End-effector position, $\mathbf{x}$ is given by the relation

$$\begin{aligned} \mathbf{x} &= \mathbf{G}_f(\mathbf{s}, \boldsymbol{\phi}, \boldsymbol{\delta}) \\ \mathbf{0} &= \boldsymbol{\Phi}(\mathbf{s}, \boldsymbol{\phi}, \boldsymbol{\delta}) \end{aligned} \tag{10}$$

where $\mathbf{G}_f(\mathbf{s}, \boldsymbol{\phi}, \boldsymbol{\delta})$ is the forward geometric model of the flexible manipulator. The objective is to find desired joint variables $\mathbf{s}_d$ for which we have $\mathbf{x}_d = \mathbf{G}_f(\mathbf{s}_d, \boldsymbol{\phi}_d, \boldsymbol{\delta}_d)$. For that purpose, we propose an iterative algorithm using manipulator static model, Eq. (11), derived from dynamic model, Eq. (3), for zero accelerations and velocities.

$$\begin{bmatrix} 0 & 0 & 0 \\ 0 & 0 & 0 \\ 0 & 0 & \mathbf{K}_\delta \end{bmatrix} \begin{bmatrix} \mathbf{s} \\ \boldsymbol{\phi} \\ \boldsymbol{\delta} \end{bmatrix} + \begin{bmatrix} \boldsymbol{\Phi}_s^T \\ \boldsymbol{\Phi}_\phi^T \\ \boldsymbol{\Phi}_\delta^T \end{bmatrix} \boldsymbol{\lambda} + \begin{bmatrix} \mathbf{g}_s \\ \mathbf{g}_\phi \\ \mathbf{g}_\delta \end{bmatrix} = \begin{bmatrix} \mathbf{u}_{eq} \\ \mathbf{0} \\ \mathbf{0} \end{bmatrix} \tag{11}$$

$\mathbf{u}_{eq}$ is the vector of control forces at equilibrium configuration. Let $\boldsymbol{\alpha}$ be a set of coordinates for which $\boldsymbol{\Phi}_\alpha$ formed from $\boldsymbol{\Phi}_q$ rows corresponding to these coordinates is square and invertible. We denote by $\mathbf{g}_\alpha$ and $\mathbf{K}_\alpha$ the vector of gravity forces and stiffness matrix corresponding to the set of coordinates $\boldsymbol{\alpha}$. To determine coordinates $\mathbf{s}_d$, $\boldsymbol{\phi}_d$ et $\boldsymbol{\delta}_d$ such that $\mathbf{x}_d = \mathbf{G}_f(\mathbf{s}_d, \boldsymbol{\phi}_d, \boldsymbol{\delta}_d)$ the following algorithm is used:

Initialization $\mathbf{s} = \mathbf{s}_r$, $\boldsymbol{\delta} = \mathbf{0}$.
Repeat
Evaluate $\boldsymbol{\phi}$ such that $\boldsymbol{\Phi}(\mathbf{s}, \boldsymbol{\phi}, \boldsymbol{\delta}) = \mathbf{0}$
$\boldsymbol{\lambda} \leftarrow \left(\boldsymbol{\Phi}_\alpha^T\right)^{-1} \left(-\mathbf{g}_\alpha(\mathbf{s}, \boldsymbol{\phi}, \boldsymbol{\delta}) - \mathbf{K}_\alpha \boldsymbol{\alpha}\right)$
$\boldsymbol{\delta} \leftarrow \mathbf{K}_\delta^{-1} \left(-\mathbf{g}_\delta - \boldsymbol{\Phi}_\delta^T \boldsymbol{\lambda}\right)$
$\boldsymbol{\varepsilon} \leftarrow \mathbf{J}_r^{-1}(\mathbf{s}) \left(\mathbf{x}_d - \mathbf{G}_f(\mathbf{s}, \boldsymbol{\phi}, \boldsymbol{\delta})\right)$
$\mathbf{s} \leftarrow \mathbf{s} + \boldsymbol{\varepsilon}$
until $|\boldsymbol{\varepsilon}| < \varepsilon_c$
$\mathbf{s}_d = \mathbf{s}$, $\boldsymbol{\phi}_d = \boldsymbol{\phi}$, $\boldsymbol{\delta}_d = \boldsymbol{\delta}$.

Evaluation of $\boldsymbol{\phi}$ is analytically possible in our case. End effector gravity compensation consists in adopting $\mathbf{s}_d$ as desired joint configuration at the end of control

4 Simulations

Simulations are performed for rigid and flexible cases. A rigid dynamic model, different (perturbed) from the one adopted for control, is also used for robustness testing: we assume that center of mass locations errors are up to 20%. For In the flexible case, retained lumped stiffness values correspond to $49Hz$ as first natural frequency and $30N/\mu m$ as minimal static stiffness. The tool reference trajectory is defined by the initial, $(0, 1200, 0)$, and the final, $(-315, 1830, 550)$, positions of the point E, units are mm, Fig. (4). Sinusoidal accelerations are imposed on each direction X, Y and Z, with respective amplitudes of $10ms^{-2}$, $20ms^{-2}$ and $20ms^{-2}$, such values are required for HSM applications. P.I.D. and inverse dynamics controllers are compared. We analyze joint space and Cartesian space tracking errors for low and high gain factors.

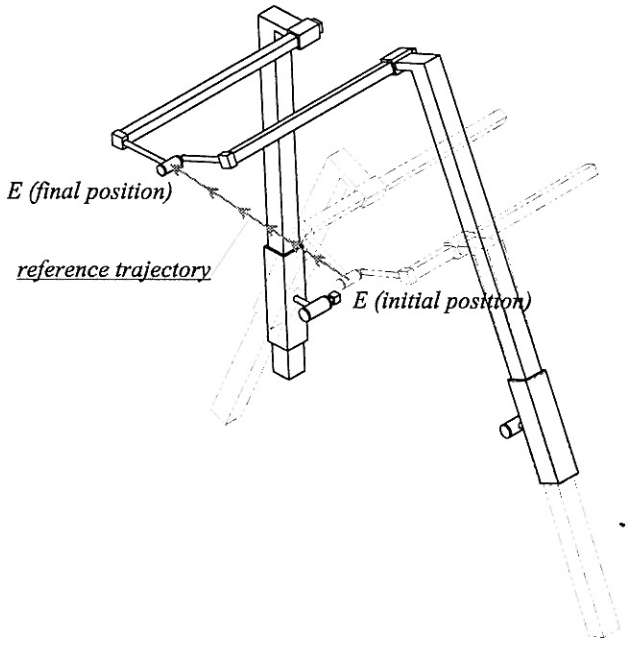

Figure 4: Cartesian reference trajectory

Simulations are performed in Matlab\Simulink® for rigid case. Because of the complexity and the size of the analytic equations, Matlab\Simulink and ADAMS\Controls® co-simulations are used for the flexible case. Pole assignment technique is used to obtain gain matrices. We adopt the same poles to compare the two control strategies. For inverse dynamics controller, pole assignement is exact. However, a mean mass value is considered for the P.I.D. controller

design.

For $k_d = 3.10^2 N.s.kg^{-1}.m^{-1}$, $k_p = 2.25\,10^3 kg^{-1}m^{-1}$ and $k_i = 3.75\,10^5 N.s^{-1}kg^{-1}.m^{-1}$, we have the evolution of joint space and cartesian space tracking errors, Fig. (5) and (6). As expected, with inversion dynamics control, tracking errors for rigid analytic model are strictly zeros since initial errors are zeros too. Computed torque control robustness is proved since tracking errors for perturbed rigid model are negligible compared to those obtained using P.I.D controller. For flexible model, maximal joint space tracking error obtained by computed torque control is less than $0.1mm$ while the one obtained by P.I.D controller is higher than $0.8mm$. Observed oscillations are less important in joint space and in cartesian space when inverse dynamic control is used.

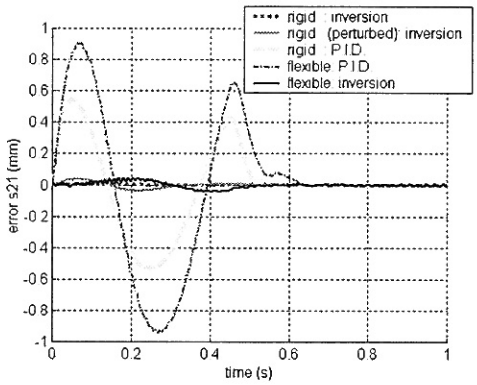

Figure 5: Joint space tracking error (s_{21}): low gains

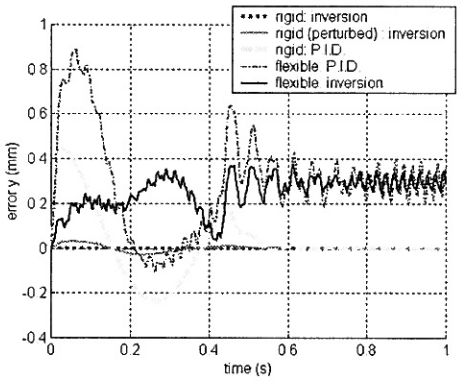

Figure 6: Cartesian space tracking error (y): low gains

By increasing gain values, $k_d = 6.10^2 N.s.kg^{-1}.m^{-1}$, $k_p = 9.10^4 N.kg^{-1}m^{-1}$ and $k_i = 3.10^6 N.s^{-1}kg^{-1}.m^{-1}$, performances in joint space are improved Fig. (7). However, oscillations in Cartesian space become more significant and affect machine stability. For the P.I.D. controller, maximal joint space tracking error is about $0.1mm$ while the one obtained by computed torque control is $0.05mm$. Observed oscillations are also higher for the P.I.D. controller, Fig. (7) and (8). In all cases, gravity forces lead to end-effector static errors due to elastic deformations. As expected, these errors are identical for both control strategies ($0.35mm$ in the Y direction). Required control forces remain acceptable and less than the maximal values for which motors are dimensioned.

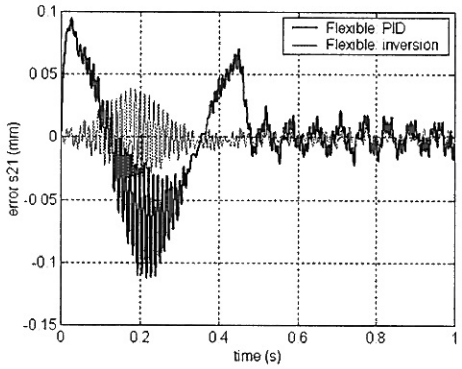

Figure 7: Joint space tracking error (s_{21}): high gains

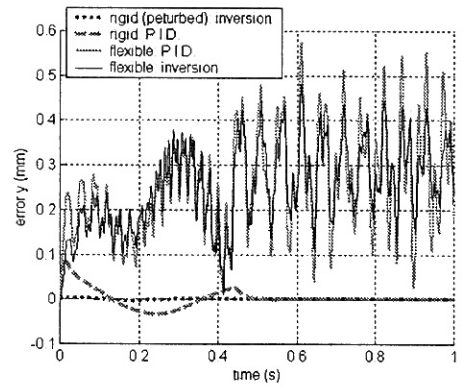

Figure 8: Cartesian space tracking error (y): high gains

By using gravity compensation algorithm described in section 3, end-effector static error are cancelled.

Compensation terms are added when tool is close to desired final position, Fig (9).

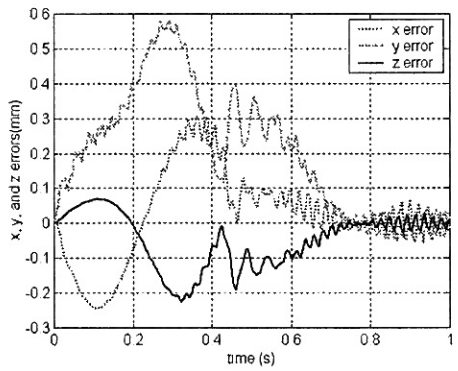

Figure 9: Gravity compensation

5 Conclusion

We have presented in this article the modeling and the control of a HSM machine tool prototype with parallel kinematics. A computed torque control was proposed and allows dynamic performances improvement compared to what one can have with a P.I.D. controller. Machine flexible behavior was considered for control validation in real applications. Simulations results show limitations due to flexibility when high gain values are adopted. An iterative algorithm was proposed to cancel steady errors raised at the tool position, due to flexibility. Algorithm convergence will be studied in further development as well as inversion control using flexible model.

References

[1] M. Aubourg, "Rapport d'étude: paramètres et réglages machines outils", Tech. Rep. CETIM, 1999.

[2] C. Boër, L. Molinari-Tosatti, and K. S. Smith, eds., *Parallel Kinematic Machines*, Great Britain: Springer-Verlag, 1999.

[3] W. J. Book, "Recurcive Lagrangian Dynamics of Flexible Manipulator Arms", *The International Journal of Robotics Research*, vol. 3, no. 3, pp. 87-101, 1984.

[4] B. C. Bouzgarrou, "Rapport Interne 2: Analyse et Commande des Mécanismes Flexibles", Tech. Rep. LaRAMA-IFMA, 2000.

[5] B. C. Bouzgarrou, P. Ray, and G. Gogu, "Static and Dynamic Characterization of New Parallel High Speed Machine Tool", *2nd International Seminar on Improving Machine Tool Performance, July 3-5, La Baule, France*, CD ROM, 2000.

[6] B. C. Bouzgarrou, P. Ray, and G. Gogu, "Manipulabilité: Critère de Synthèse de Manipulateurs Parallèle Plans", *3rd International Conference IDMME'2000, May 16-19, Montréal, Canada*, 2000.

[7] C. Canudas de Wit, B. Siciliano, and G. Bastin, eds., *Theory of Robot Control*. Great Britain: Springer-Verlag, 1996.

[8] G. Gogu, P. Coiffet, and A. Barraco, *Représentation des Déplacements des Robots* .Paris: Hermes, 1997.

[9] C. J. Li and T. S. Shankar, "Systematic Methods for Efficient Modeling and Dynamics Computation of Flexible Robot Manipulators", *IEEE Transactions on system, man, and cybernetics*, vol. 23, no.1, pp. 77-95, 1993.

[10] J. P. Merlet, *Les Robots Parallèles*, Paris, Hermes 1997.

[11] P. Poignet, M. Gautier, and W. Khalil, "Modeling, Control, and Simulation of High Speed Machine Tool Axes", *Int. Conf. on Advanced Intelligent Mechatronics, September 19-23, Atlanta, USA*, pp. 617-622, 1999.

[12] A. A. Shabana, *Dynamics of Multibody Systems*. USA: Cambridge University Press, 1998.